PACS numbers: 42.60.Jf; 52.50.Jm
DOI: 10.1070/QE2001v031n11ABEH002085

Spatiotemporal smoothing of a laser beam employing a dynamic plasma phase plate

I N Voronich, S G Garanin, V N Derkach, A I Zaretskii, A G Kravchenko, V A Lebedev, A V Pinegin, A V Sosipatrov, S A Sukharev

***Abstract*. The spatiotemporal smoothing of the intensity distribution of a focused laser beam was investigated on the Iskra-4 laser setup using a dynamic plasma phase plate produced by vaporisation of a special target placed at the beginning of the caustic of the focused beam. It is shown that the transmittance of the plasma target in the $10^{13} - 2 \times 10^{14}$ W cm^{-2} intensity range is no less than 70 % – 80 %. The introduction of the dynamic plasma phase plate lowered the relative fluctuations of the spatial intensity distribution from 100 % to ~ 10 %. The characteristic time of the intensity distribution variation in the focal plane is 0.4 ps.**

Keywords: *nonuniform irradiation, intensity distribution, spatiotemporal smoothing, dynamic plasma phase plate.*

1. Introduction

The spatiotemporal smoothing (STS) of laser beams is of critical importance in the solution of the problem of spherically symmetric compression of direct-irradiation targets on high-power multiple-beam laser facilities employed in laser fusion research. The mutual interference of the beams and the aberrations of each beam at the output of the amplification channel are responsible for a speckle intensity distribution $J(r)$ in the focal region with a modulation depth up to 100 %. The target irradiation nonuni-formity arising in this case can favour the development of hydrodynamic instabilities, which disturb the symmetry of compression.

The basic idea of obtaining a smooth intensity distribution $I(r)$ is to use the additional STS to accomplish a rapid transformation of the speckle distribution in time. In this case, the hydrodynamic plasma motion should not manage to react to the 'flickering' spots of enhanced laser radiation intensity. If the characteristic transformation time $t_0 \leqslant t_h = 1 - 10$ ps, where t_h is the hydrodynamic plasma response time, the plasma motion will not be able to react to the instantaneous intensity distribution $J(r, t)$ and will be determined by the distribution

$$I(r) = \frac{1}{t_h} \int_0^{t_h} J(r, t) \mathrm{d}t$$

integrated over the time t_h.

Special STS methods have been elaborated to date, such as production of induced spatial incoherence [1], smoothing by spectral dispersion [2], and others [3, 4], wherein the basic idea consists in the disturbance of spatial coherence of the beams. In these methods, the characteristic transformation time of $J(r, t)$ is determined by the coherence time $t_c \sim 1/\Delta\nu_0$, where $\Delta\nu_0$ is the spectral width of laser radiation.

The time required for achieving the desired irradiation uniformity by these methods is rather long, amounting to 0.5 – 1 ns [5, 6]. On the other hand, these methods are inapplicable for high-power photodissociation Iskra-4 and Iskra-5 lasers with an extremely narrow amplification band $\Delta\nu \sim 10^8 - 10^9$ Hz, for which $t_c \gg t_h$. The authors of Ref. [7] proposed to use a dynamic plasma phase plate (DPPP) for STS located directly in the focal region and representing a transient plasma cloud through which a laser beam propagates (Fig. 1). For specific plasma parameters (density ρ, temperature T, expansion velocity V), the wave front of the laser beam at the exit from the plasma will experience a strong deformation in time, which can result in the transformation of $J(r, t)$ in the next half-space along the beam propagation.

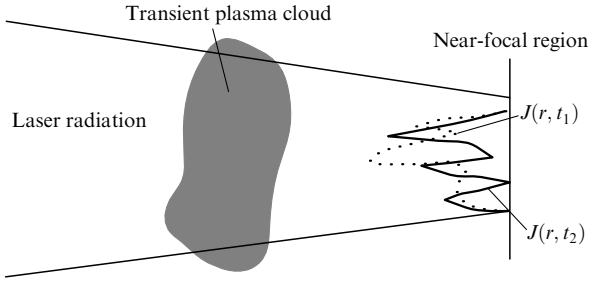

Figure 1. Schematic of the spatiotemporal smoothing of laser radiation using a transient plasma.

Estimates [7] of the parameters of a transient plasma producing STS show that for a plasma temperature $T_e \geqslant 100$ eV, density $\rho \approx 0.1\rho_{cr}$ (ρ_{cr} is the critical density), and optical thickness $k_0 L \sim 100$ ($k_0 = 2\pi/\lambda$, L is the longitudinal plasma dimension, and λ is the wavelength of laser radiation), the energy loss of the laser pulse does not exceed 20 %. In this case, the characteristic variation time of the

I N Voronich, S G Garanin, V N Derkach, A I Zaretskii, A G Kravchenko, V A Lebedev, A V Pinegin, A V Sosipatrov, S A Sukharev Russian Federal Nuclear Centre, All-Russian Research Institute of Experimental Physics, prospekt Mira 37, 607190 Sarov, Nizhnii Novgorod oblast, Russia

Received 12 July 2001
Kvantovaya Elektronika **31** (11) 970–972 (2001)
Translated by E N Ragozin

nonuniformity of plasma density profile should be less than 10 ps. In this work, we verified for the first time the possibility of laser beam smoothing by means of a DPPP.

2. Experimental

The study was performed using an Iskra-4 laser setup [8]. To produce the basic intensity distribution $I_0(r)$, we employed a random phase plate [9]. A schematic of the experiment is shown in Fig. 2. We used two counterpropagating laser beams. The optical scheme with two radiation beams allows us, first, to introduce the time delay Δt for the pulse arrival at the target (the version with a prepulse) and, second, to irradiate a target simultaneously at two wavelengths.

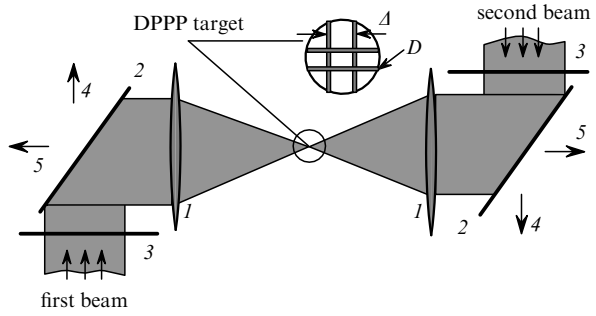

Figure 2. Schematic of the experiment and the enlarged fragment of the target (inset):
(*1*) camera objectives with the focal length $F = 60$ cm; (*2*) dielectric mirrors; (*3*) phase plates; (*4*, *5*) directions of diagnostics of parameters of the incident radiation and radiation transmitted through the DPPP, respectively; (D) fibre thickness; (Δ) fibre separation.

We used the second-harmonic radiation from an iodine photodissociation laser at 0.657 μm in both beams. Objectives (*1*) were so positioned that the DPPP was located at the beginning of the caustic of both focused radiation beams. Experiments were performed with a DPPP target in the form of a two-dimensional equidistant set of fibres of a CH-like material with the density $\rho \sim 1$ g cm^{-3} (Fig. 2). The set consisted of four pairwise crossed fibres of thickness $D = 1.8 - 2.4$ μm (in several cases up to 4 μm) spaced $\Delta = 180 - 220$ μm apart.

The energy of the first beam (the high-power plasma-producing beam) was up to 50 J per pulse. The second (diagnostic) beam delivered an energy of 15 J per pulse and was delayed relative to the first one by Δt; the delay being varied between zero and 250 ps. The pulse duration for both beams was $\tau_{0.5} = 0.3 - 1.0$ ns, the energy and power contrast ratios were higher than 10^7, the divergence θ was 5×10^{-4} rad taking the phase plate into account, the size of the spot at the target was 300 – 350 μm, the transverse accuracy of the spot falling on the target being $\delta_\perp \leqslant 60$. The maximum intensity of the second radiation beam at the DPPP did not exceed 2×10^{14} W cm^{-2} for $\tau_{0.5} \sim 0.5$ ns and $\Delta t = 0$.

The parameters of initial radiation were recorded in the experiments: the energy and the duration of a laser pulse, the energy and power contrast ratios, the near- and far-field beam structures, and the intensity distribution in near-focal planes in the absence of a DPPP. For the laser radiation transmitted through the DPPP, we recorded the target transmittance (in the solid angle corresponding to the angles of convergence of the incident radiation), the spectrum and the intensity distribution of laser radiation in the focal plane with a time resolution, and the integrated intensity distribution in the focal plane.

The integrated intensity distribution was recorded by a photographic technique. The spectral characteristics of laser radiation were measured with a monochromator with a 600 lines mm^{-1} reflection diffraction grating and a fast streak camera [10] with a time resolution of 20 ps. The instrument function of the measuring complex was $\sim 8 - 10$ Å and the rms resolution of the spectral signal was about 2 Å. The intensity distribution in the focal plane was recorded with a time resolution of 10 ps. The spatial resolution of the recorded signal reduced to the focal plane was 0.5 μm for a characteristic diffraction-limited dimension of the focused beam of ~ 4 μm.

3. Experimental results

The typical form of the integrated intensity distribution in the focal plane, which is determined by the phase plate used, is shown in Fig. 3a for the experiment performed in the absence of a DPPP. The introduction of the DPPP into the prefocal region results in the smoothing of the speckle intensity distribution $I_0(r)$ of the laser beam because of the phase modulation in the transient plasma (Fig. 3b). A comparison of the distributions in Figs 3a and 3b shows that the use of the DPPP reduces the speckle modulation depth from ~ 100 % to ~ 10 %. In this case, the effect is observed in a wide intensity range of the plasma-producing beam ($10^{13} - 2 \times 10^{14}$ W cm^{-2}). The DPPP transmittance recorded in this intensity range is 70 % – 80 %.

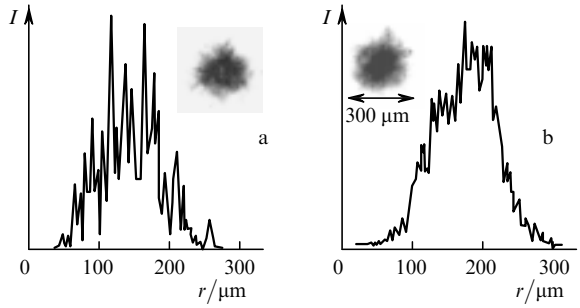

Figure 3. Intensity distribution in the focal plane without (a) and with (b) the use of a DPPP, and radiation spot shapes (at the top).

The results of measurements of integrated distributions $I(r)$ are consistent with the structure dynamics of the intensity distribution $I^*(r, t)$ in the focal plane measured after the radiation interaction with the DPPP (Fig. 4). The distribution $I_0^*(r, t)$ recorded in the absence of the DPPP (Fig. 4a) shows that the initial laser beam has a clearly defined speckle character during the laser pulse.

The distribution $I^*(r, t)$ obtained using the DPPP is substantially different. Fig. 4b shows a typical intensity distribution for the diagnostic beam in the focal plane recorded with the 150-ps delay of the diagnostic beam relative to the high-power beam. Figs 4c – 4f show the results of image processing in the sections corresponding to different points in time. One can see that early in the pulse (Fig. 4c) the beam structure is strongly speckled. However, within 70 ps after the onset of the diagnostic beam the speckle structure begins

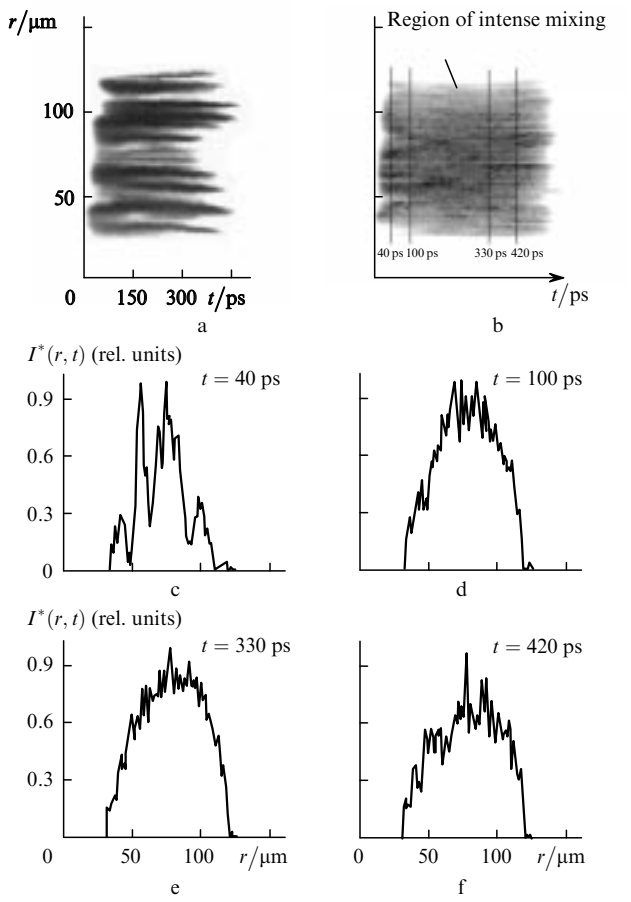

Figure 4. Time-resolved intensity distribution in a part of the cross section of the diagnostic beam in the focal plane in an experiment without (a) and with (b) the use of the DPPP, and the intensity distributions at different points in time t after the onset of the pulse (c–f) in the case when the DPPP was employed.

to break down, and the cross-sectional intensity distribution of laser radiation is nearly smooth over an interval approximately 300 ps long (Figs 4d–4f). Later on, the speckles begin to partly restore at the trailing edge of the pulse (Fig. 4f).

Note that integration of the distributions with respect to time

$$I_{\mathrm{t}}^{*}(r) = \int_0^{\infty} I^{*}(r,t)\mathrm{d}t$$

yields a distribution which agrees well with the results of integral recording $I(r)$ (Fig. 3b). In particular, the modulation depth of $I_{\mathrm{t}}^{*}(r)$ is $\sim 10\,\%$.

The measured modulation depth of $I^{*}(r,t)$ at the instant of strongest smoothing (see Figs 4d and 4e) was $5\,\%-10\,\%$. The distributions obtained are in fact integrated over the resolution time Δt_{p} of the detector:

$$I^{*}(r,t) = \frac{1}{\Delta t_{\mathrm{p}}}\int_{t-\Delta t_{\mathrm{p}}/2}^{t+\Delta t_{\mathrm{p}}/2} J(r,t)\mathrm{d}t,$$

where $\Delta t_{\mathrm{p}} = 10$ ps and $J(r,t)$ is the instantaneous intensity distribution. An analysis of $I^{*}(r,t)$ shows that the obtained modulation depth can be attributed to the reconstruction of $J(r,t)$ with the characteristic time $\Delta t^{*} \sim 0.4-0.5$ ps [11, 12].

The obtained time Δt^{*} correlates well with the spectrum of laser radiation recorded after its passage through the DPPP (Fig. 5). The measured width of the emission spectrum is $\Delta\nu \sim 2.5\times 10^{12}$ Hz (for the initial $\Delta\nu_0 < 10^9$ Hz), i.e. $\Delta\nu \sim 1/\Delta t^{*}$. In this case, the main features of the spectrum being recorded are the spectral width of 25–40 Å throughout the intensity range of laser radiation irradiating the target, the red shift of the spectrum, and the characteristic time (up to 0.5 ns) during which the measured spectrum width exceeds the instrumental function width.

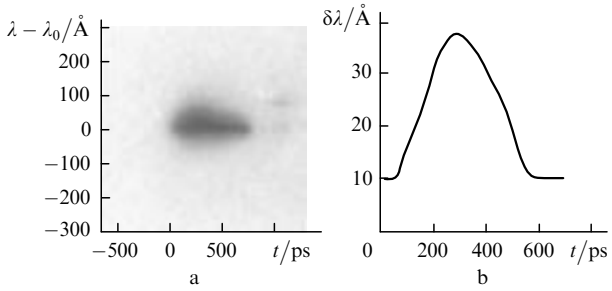

Figure 5. Streak photograph of the spectrum of radiation transmitted through the DPPP (a) and the time dependence of the local width of the radiation spectrum at a level of 0.5 of the maximum spectral signal intensity at the point in time t (b).

Acknowledgements. This work was partly supported by the Russian Foundation for Basic Research (Grant No. 00-15-96730).

References

1. Lehmberg R H, Obenschain S P *Opt. Commun.* **46** 27 (1983)
2. Scupsky S, Short R W, et al. *J. Appl. Phys.* **66** 3456 (1989)
3. Phase Conversion Using Distributed Polarization Rotation *LLE Review* **45** 1 (1990)
4. Nakano N, Tsubakimoto K, et al. *J. Appl. Phys.* **73** 2122 (1993)
5. Two-Dimensional SSD on OMEGA *LLE Review* **69** 1 (1996)
6. Demonstration of Dual-Tripler, Broadband Third-Harmonic Generation and Implications for Omega and the NIF *LLE Review* **75** 151 (1999)
7. Bessarab A V, Derkach V N, et al. *Proc. SPIE Int. Soc. Opt. Eng.* **2767** 97 (1995)
8. Zaretskii A I, Kirillov G A, et al. *Kvantovaya Elektron.* **10** 756 (1983) [*Sov. J. Quantum Electron.* **13** 468 (1983)]
9. Kato Y, Mimo K, et al. *Phys. Rev. Lett.* **53** 1057 (1984)
10. Murugov V M, Okutin G P, et al. *Prib. Tekh. Eksp.* (2) 155 (1993)
11. Bondarenko S V, Garanin S G, et al. *Kvantovaya Elektron.* **26** 237 (1999) [*Quantum Electron.* **29** 237 (1999)]
12. Derkach V N, Bondarenko S V, et al. *Laser Part. Beams* **17** 603 (1999)